Analyzing Coverage Probability in Full-Duplex Two-Tier Networks with Offloading and Resource Partitioning

Mehrdad Salimnejad*, William Tärneberg†, Christian Nyberg †, and Nikolaos Pappas*
*Department of Computer and Information Science, Linköping University, Linköping, Sweden
†Department of Electrical and Information Technology, Lund University, Lund, Sweden
{mehrdad.salimnejad, nikolaos.pappas}@liu.se, {william.tarneberg, christian.nyberg@eit.lth.se}

***Abstract*—Full-duplex (FD) communication improves spectral efficiency by allowing simultaneous transmission and reception on the same frequency band. This paper analyzes a two-tier network consisting of macrocells and picocells, where base stations (BSs) operate in FD mode while users operate in half-duplex (HD) mode. However, interference remains a major challenge in these systems, significantly impacting coverage probability. To enhance network performance, we incorporate user offloading and resource partitioning. Offloading redistributes users from macrocells to picocells to balance the network load. However, offloaded users often experience lower SINR compared to those connected to macrocells. Resource partitioning is applied to mitigate this SINR degradation and reduce interference. This method allocates a fraction of time or frequency resources where macrocells remain inactive, allowing picocells to serve users with less interference. We derive analytical expressions for the downlink coverage probability, considering the effects of offloading, resource partitioning, and key network parameters. Our results indicate that load balancing by itself is insufficient; however, when resource partitioning is combined with offloading, DL coverage probability is significantly improved.**

I. Introduction

Heterogeneous Cellular Networks (HCNs) consist of macro base stations (BSs) and various low-power small BSs, including microcells, picocells, and femtocells [1]–[4]. Most user equipments (UEs) in these networks are typically associated with high-power BSs. As a result, the coverage areas of low-power small BSs are significantly smaller than those of macro BSs, leading to an imbalance in load distribution among BSs. This uneven load distribution often causes macro BSs to become overloaded, resulting in suboptimal rate allocation across the network and Quality of Service (QoS) degradation due to limited resources [5], [6]. Cell range expansion (CRE) [3] is a technique designed to enhance the coverage area of low-power small cells. In this approach, user equipment (UE) is offloaded to a low-power base station (BS) when the difference in received signal strength between the macro and small BSs falls within a predefined bias threshold. While CRE improves load balancing and mitigates network congestion, it also increases co-channel interference for offloaded UEs, as the strongest macro BS contributes to the interference [5]. A method to reduce interference is resource partitioning [3], [7], in which the macro tier transmission is periodically muted over a portion of the radio resources. This enables small cells to schedule offloaded users in these muted resources, protecting them from co-channel interference. The study in [8] analyzed the impact of offloading in HCNs and derived analytical expressions for the SINR distribution and the spectral efficiency of UEs associated with macro and small cells. In [9], the authors examined the effect of resource partitioning in HCNs and derived analytical expressions for the SINR and throughput. The effect of resource partitioning and offloading in HCNs was studied in [10], but the analysis considered only downlink (DL) transmission. To improve the rate distribution across the network, [10] examined joint resource partitioning and offloading for DL rate distribution in a two-tier cellular network, where each tier's BSs were modeled as an infinite two-dimensional Poisson point process (2D-PPP). In addition, it was assumed that UEs are distributed according to an independent 2D-PPP. Full-duplex (FD) radios have emerged as a promising technology for next-generation wireless networks, providing better spectral efficiency than traditional half-duplex (HD) systems. By enabling simultaneous DL and uplink (UL) transmissions in the same frequency band, FD systems can significantly enhance spectral efficiency, resulting in more efficient wireless communication [11]–[13]. In [14], the authors derived the throughput of a hybrid FD/HD system considering BS spatial density, self-interference cancellation capability, and transmission power of BSs and UEs. The work in [15] employs stochastic geometry to examine the spectral efficiency and coverage probability of an FD millimeter-wave (mmWave) system, where beamforming at BSs and UEs reduces co-channel interference (CCI). However, these studies have not examined the impact of offloading and resource partitioning on FD systems. Motivated by [10], in this work, we study a two-tier HCN where BSs employ FD operation while UEs operate in HD mode. The spatial distributions of BSs and UEs are modeled using independent 2D-PPP with constant intensity. All communication channels are subject to Rayleigh fading and path loss. We derive analytical expressions for the DL coverage probability with resource partitioning as a function of power control and offloading for a randomly chosen mobile UE.

This work has been supported in part by the Swedish Research Council (VR), and ELLIIT.

ISBN 978-3-903176-73-7

II. System Model

This work considers a wireless cellular network with a two-tier deployment of BSs. We assume that the locations of the BSs in the kth tier ($k = 1, 2$) follow a homogeneous 2D-PPP $\Phi_{\mathrm{B},k}$ with density $\lambda_{\mathrm{B},k}$, where all BSs operate in FD mode. The first tier consists of macrocells, while the second tier consists of picocells. Additionally, UEs are independently distributed according to a homogeneous 2D-PPP Φ_{U} with density $\lambda_{\mathrm{U}} > \lambda_{\mathrm{B},k}$, and they operate in HD mode. In FD mode, both DL and UL directions are assumed to be available, whereas in HD mode, only the UL direction is available. Additionally, it is assumed that the nearest BS serves each UE. In [16], it was shown that the distance between a randomly chosen UE and its closest BS in the kth tier, denoted by R_k, follows a Rayleigh distribution. Thus, its probability density function (PDF) can be written as:

$$f_{R_k}(r) = 2\pi\lambda_{\mathrm{B},k} r e^{-\pi\lambda_{\mathrm{B},k} r^2}, r \geqslant 0. \tag{1}$$

In this paper, it is assumed that transmission channels are subject to Rayleigh fading and path loss. For BS-UE and UE-UE in kth tier, path loss is given by $G_{\mathrm{BU},k} r^{-\alpha_{\mathrm{BU},k}}$ and $G_{\mathrm{UU},k} r^{-\alpha_{\mathrm{UU},k}}$, respectively, in which $\alpha_{\mathrm{BU},k}$ and $\alpha_{\mathrm{UU},k}$ are the path loss exponents and $G_{\mathrm{BU},k}$ and $G_{\mathrm{UU},k}$ are constant values depending on the system parameters such as antenna gain. Furthermore, fading powers for the BS-UE and UE-UE links are denoted by H and Q, respectively, and they are jointly independent and identically distributed (i.i.d.) random variables (RVs) with unit mean. We assume that the transmit power of every BS of kth tier over bandwidth W is fixed and equals $P_{\mathrm{B},k}$. In addition, we consider distance proportional fractional power control for UL directions to compensate for path loss [17]. Therefore, the transmit power of each UE in kth tier is equal to $P_{\mathrm{U},k}(R_k) = \min\left\{\rho G_{\mathrm{BU},k}^{-\epsilon} R_k^{\epsilon\alpha_{\mathrm{BU},k}}, P_{\max}\right\}$, where $\epsilon \in [0, 1]$ is the power control factor, ρ is the desired received power at BS of kth tier, provided that the path loss is fully compensated and $P_{\max}$ is the maximum power transmit at UE [18]. The average received power at the BS of the kth tier is given by $\rho R_k^{(\epsilon-1)\alpha_{\mathrm{BU},k}}$ for $0 \leqslant R_k < y$, and by $P_{\max} G_{\mathrm{BU},k} R_k^{\alpha_{\mathrm{BU},k}}$ for $R_k \geqslant y$, where

$$y = \left(P_{\max} G_{\mathrm{BU},k}/\rho\right)^{\frac{1}{\epsilon\alpha_{\mathrm{BU},k}}}. \tag{2}$$

A. User Association Scheme

For the analysis, we assume that a typical user at the origin, denoted by u_o, is associated with the strongest BS in the kth tier based on the maximum received power [10]. The maximum received power is given by

$$P_{r,k} = P_{\mathrm{B},k} G_{\mathrm{BU},k} R_k^{-\alpha_{\mathrm{BU},k}}, \tag{3}$$

where R_k denotes the distance from the origin to the strongest BS in the kth tier. In (3), the fading effect is neglected to avoid the ping-pong handover effect [19]. Based on the maximum received power from each tier, a typical user at the origin is associated with the strongest BS in the kth tier and classified into three disjoint sets [10].

$$u_o \in \begin{cases} \mathcal{U}_m & , P_{r,1} \geqslant \mathcal{B} P_{r,2}, \\ \mathcal{U}_e & , P_{r,2} \leqslant P_{r,1} < \mathcal{B} P_{r,2}, \\ \mathcal{U}_p & , P_{r,1} < P_{r,2}, \end{cases} \tag{4}$$

where $\mathcal{B}$ is the association bias introduced for the second tier (picocells). According to (4), when $P_{r,1} \geqslant \mathcal{B} P_{r,2}$, the typical user is associated with macrocells, and when $P_{r,1} < P_{r,2}$, it is associated with picocells. Otherwise, if $P_{r,2} \leqslant P_{r,1} < \mathcal{B} P_{r,2}$, the typical user is offloaded from macrocells to picocells due to cell range expansion, and in this case, macrocells are assumed to be muted. In (4), we define $\Phi_{\mathrm{U},1}$ as the sets of users associated with macrocell, $\Phi_{\mathrm{U},2}$ as the sets of users associated with picocell and Φ^e is the sets of users associated with range-expanded picocell, where $\Phi_{\mathrm{U}} = \Phi_{\mathrm{U},1} \cup \Phi_{\mathrm{U},2} \cup \Phi^e$.

B. Resource Partitioning Approach

Resource partitioning is a technique in which the macrocell suspends transmission over a fraction of time or frequency resources, allowing the picocell to schedule range-expanded users on these resources while mitigating interference from the macrocell. We define the resource partitioning fraction as μ, where $0 < \mu < 1$ represents the portion of resources during which the macrocell remains inactive. Accordingly, in the remaining fraction, $1 - \mu$, the macrocell allocates its available resources to users in $\mathcal{U}_m$, while the picocell assigns its resources to users in $\mathcal{U}_p$.

III. Downlink Coverage Probability

In this section, we derive the DL coverage probability in a FD two-tier cellular network, which is defined as the complementary cumulative distribution function (CCDF) of the SINR contribution from a randomly chosen UE.

A. Mathematical Derivation

The downlink SINR of a randomly selected UE in a FD two-tier cellular network is given by

$$\mathrm{SINR} = \begin{cases} \frac{P_{\mathrm{B},1} H_o G_{\mathrm{BU},1} R_1^{-\alpha_{\mathrm{BU},1}}}{\sum_{k=1}^{2} I_{m,k} + \sigma_{\mathrm{U}}^2} & , u_o \in \mathcal{U}_m, \\ \frac{P_{\mathrm{B},2} H_o G_{\mathrm{BU},2} R_2^{-\alpha_{\mathrm{BU},2}}}{\sum_{k=1}^{2} I_{p,k} + \sigma_{\mathrm{U}}^2} & , u_o \in \mathcal{U}_p, \\ \frac{P_{\mathrm{B},2} H_o G_{\mathrm{BU},2} R_2^{-\alpha_{\mathrm{BU},2}}}{I_e + \sigma_{\mathrm{U}}^2} & , u_o \in \mathcal{U}_e, \end{cases} \tag{5}$$

where, σ_{U}^2 represents the variance of the complex additive white Gaussian noise (AWGN) at the UE, $\mathrm{B}_o \in \mathbb{R}^2$ denotes the location of the serving BS, and H_o is the fading power between the desired UE and its serving BS. Additionally, $I_{m,k}$, $I_{p,k}$, and I_e represent the total interference affecting the desired UE from all UL-UEs and all BSs operating in the DL direction, depending on whether the desired UE belongs to macrocell users, picocell users, or range-expanded picocell users, respectively. These interferences are defined as follows:

$$I_{m,k} = \sum_{\mathrm{B}_j \in \Phi_{\mathrm{B},k}\setminus\{\mathrm{B}_o\}} P_{\mathrm{B},k} G_{\mathrm{BU},k} H_j L_j^{-\alpha_{\mathrm{BU},k}} + \sum_{u_j \in \Phi_{\mathrm{U},k}\setminus\{u_o\}} P_{\mathrm{U},k}\left(R_j\right) Q_j G_{\mathrm{UU},k} D_j^{-\alpha_{\mathrm{UU},k}}, \quad (6)$$

$$I_{p,k} = \sum_{\mathrm{B}_j \in \Phi_{\mathrm{B},k}\setminus\{\mathrm{B}_o\}} P_{\mathrm{B},k} G_{\mathrm{BU},k} H_j L_j^{-\alpha_{\mathrm{BU},k}} + \sum_{u_j \in \Phi_{\mathrm{U},k}\setminus\{u_o\}} P_{\mathrm{U},k}\left(R_j\right) Q_j G_{\mathrm{UU},k} D_j^{-\alpha_{\mathrm{UU},k}}, \quad (7)$$

$$I_{e} = \sum_{\mathrm{B}_j \in \Phi_{\mathrm{B},2}\setminus\{\mathrm{B}_o\}} P_{\mathrm{B},2} G_{\mathrm{BU},2} H_j L_j^{-\alpha_{\mathrm{BU},2}} + \sum_{u_j \in \Phi_{\mathrm{U}}^{e}\setminus\{u_o\}} P_{\mathrm{U},2}\left(R_j\right) Q_j G_{\mathrm{UU},2} D_j^{-\alpha_{\mathrm{UU},2}}, \quad (8)$$

where L_j represents the distance between the desired UE and the jth BS in the kth tier, where $\mathrm{B}_j \in \Phi_{\mathrm{B},k} \setminus \{\mathrm{B}_o\}$. Additionally, D_j denotes the distance between the desired UE and the jth interfering UE in the kth tier, with $u_j \in \Phi_{\mathrm{U},k} \setminus \{u_o\}$. Furthermore, R_j refers to the distance between the jth UL-UE and its corresponding serving BS in the kth tier, where $u_j \in \Phi_{\mathrm{U},k} \setminus \{u_o\}$. We assume that $\{R_j\}$ are i.i.d. RVs following a Rayleigh distribution, with the PDF given by (1). Additionally, H_j and Q_j represent the fading powers between the jth BS and the desired UE, and between the desired UE and the jth interfering UE in the kth tier, respectively. $\{H_j\}$ and $\{Q_j\}$ are jointly i.i.d RVs with a unit mean. Now, using the total probability theorem, the CCDF of the DL SINR for a randomly chosen UE in a FD two-tier cellular network is given by

$$\begin{aligned}\Pr\left[\mathrm{SINR} > \gamma_{\mathrm{th}}\right] &= \Pr\left[\mathrm{SINR} > \gamma_{\mathrm{th}} \middle| u \in \mathcal{U}_m\right]\Pr\left[u \in \mathcal{U}_m\right] \\ &+ \Pr\left[\mathrm{SINR} > \gamma_{\mathrm{th}} \middle| u \in \mathcal{U}_p\right]\Pr\left[u \in \mathcal{U}_p\right] \\ &+ \Pr\left[\mathrm{SINR} > \gamma_{\mathrm{th}} \middle| u \in \mathcal{U}_e\right]\Pr\left[u \in \mathcal{U}_e\right]. \quad (9)\end{aligned}$$

Lemma 1. *The associate probabilities* $\Pr\left[u \in \mathcal{U}_m\right]$, $\Pr\left[u \in \mathcal{U}_p\right]$, *and* $\Pr\left[u \in \mathcal{U}_e\right]$ *in* (9) *are given by*

$$\begin{aligned}\Pr\left[u\in\mathcal{U}_m\right] &= \int_0^\infty 2\pi\lambda_{\mathrm{B},1} r \exp\left[-\pi\sum_{k=1}^{2}\lambda_{\mathrm{B},k} T_1^{\frac{2}{\alpha_{\mathrm{BU},k}}} r^{\frac{2\alpha_{\mathrm{BU},1}}{\alpha_{\mathrm{BU},k}}}\right]\mathrm{d}r, \\ \Pr\left[u \in \mathcal{U}_p\right] &= \int_0^\infty 2\pi\lambda_{\mathrm{B},2} r \exp\left[-\pi\sum_{k=1}^{2}\lambda_{\mathrm{B},k} T_2^{\frac{2}{\alpha_{\mathrm{BU},k}}} r^{\frac{2\alpha_{\mathrm{BU},2}}{\alpha_{\mathrm{BU},2}}}\right]\mathrm{d}r, \\ \Pr\left[u \in \mathcal{U}_e\right] &= \int_0^\infty 2\pi\lambda_{\mathrm{B},2} r \left\{\exp\left[-\pi\sum_{k=1}^{2}\lambda_{\mathrm{B},k} T_3^{\frac{2}{\alpha_{\mathrm{BU},k}}} r^{\frac{2\alpha_{\mathrm{BU},2}}{\alpha_{\mathrm{BU},k}}}\right] \right. \\ &\left. - \exp\left[-\pi\sum_{k=1}^{2}\lambda_{\mathrm{B},k} T_2^{\frac{2}{\alpha_{\mathrm{BU},k}}} r^{\frac{2\alpha_{\mathrm{BU},2}}{\alpha_{\mathrm{BU},k}}}\right]\right\}\mathrm{d}r, \quad (10)\end{aligned}$$

where $T_1 = \frac{P_{\mathrm{B},k}G_{\mathrm{BU},k}\mathcal{B}^k}{P_{\mathrm{B},1}G_{\mathrm{BU},1}\mathcal{B}}$, $T_2 = \frac{P_{\mathrm{B},k}G_{\mathrm{BU},k}}{P_{\mathrm{B},2}G_{\mathrm{BU},2}}$, *and* $T_3 = \frac{P_{\mathrm{B},k}G_{\mathrm{BU},k}\mathcal{B}^k}{P_{\mathrm{B},2}G_{\mathrm{BU},2}\mathcal{B}^2}$.

Proof: See Appendix A. ∎

Lemma 2. *The conditional probabilities in* (9) *are given by*

$$\begin{aligned}&\Pr\left[\mathit{SINR} > \gamma_{\mathrm{th}} \middle| u \in \mathcal{U}_m\right] \\ &= \int_0^\infty \frac{2\pi\lambda_{\mathrm{B},1} r}{\Pr\left[u\in\mathcal{U}_{\mathrm{m}}\right]} \exp\left[-\left(\pi\sum_{k=1}^{2}\lambda_{\mathrm{B},k}\left(\frac{P_{\mathrm{B},k}G_{\mathrm{BU},k}}{P_{\mathrm{B},1}G_{\mathrm{BU},1}}\right)^{\frac{2}{\alpha_{\mathrm{BU},k}}} r^{\frac{2\alpha_{\mathrm{BU},1}}{\alpha_{\mathrm{BU},k}}} \right.\right. \\ &\left.\left. \times \Phi\left(\gamma_{\mathrm{th}}, \alpha_{\mathrm{BU},k}, \frac{\mathcal{B}^k}{\mathcal{B}}\right) + \eta_1\sigma_{\mathrm{U}}^2\right)\right] \prod_{k=1}^{2} g\left(\eta_1, \tau_k, k\right)\mathrm{d}r, \quad (11)\end{aligned}$$

$$\begin{aligned}&\Pr\left[\mathit{SINR} > \gamma_{th} \middle| u \in \mathcal{U}_p\right] \\ &= \int_0^\infty \frac{2\pi\lambda_{\mathrm{B},2} r}{\Pr\left[u \in \mathcal{U}_p\right]} \exp\left[-\left(\pi\sum_{k=1}^{2}\lambda_{\mathrm{B},k} T_2^{\frac{2}{\alpha_{\mathrm{BU},k}}} r^{\frac{2\alpha_{\mathrm{BU},2}}{\alpha_{\mathrm{BU},k}}} \right.\right. \\ &\left.\left. \times \Phi\left(\gamma_{\mathrm{th}}, \alpha_{\mathrm{BU},k}, 1\right) + \eta_2\sigma_{\mathrm{U}}^2\right)\right] \prod_{k=1}^{2} g\left(\eta_2, \tau_k, k\right)\mathrm{d}r, \quad (12)\end{aligned}$$

$$\begin{aligned}&\Pr\left[\mathit{SINR} > \gamma_{th} \middle| u \in \mathcal{U}_e\right] \\ &= \int_0^\infty \frac{2\pi\lambda_{\mathrm{B},2} r}{\Pr\left\{u \in \mathcal{U}_e\right\}} \exp\left[-\left(\pi\lambda_{\mathrm{B},2} r^2 \Phi\left(\gamma_{\mathrm{th}}, \alpha_{\mathrm{BU},2}, 1\right) + \eta_2\sigma_{\mathrm{U}}^2\right)\right] \\ &\times\left\{\exp\left[-\pi\lambda_{\mathrm{B},1}\left(\frac{P_{\mathrm{B},1}G_{\mathrm{BU},1}}{P_{\mathrm{B},2}G_{\mathrm{BU},2}\mathcal{B}}\right)^{\frac{2}{\alpha_{\mathrm{BU},1}}} r^{\frac{2\alpha_{\mathrm{BU},2}}{\alpha_{\mathrm{BU},1}}}\right] \right. \\ &\left. - \exp\left[-\pi\lambda_{\mathrm{B},1}\left(\frac{P_{\mathrm{B},1}G_{\mathrm{BU},1}}{P_{\mathrm{B},2}G_{\mathrm{BU},2}}\right)^{\frac{2}{\alpha_{\mathrm{BU},1}}} r^{\frac{2\alpha_{\mathrm{BU},2}}{\alpha_{\mathrm{BU},1}}}\right]\right\} g\left(\eta_2, \tau_2, k\right)\mathrm{d}r, \quad (13)\end{aligned}$$

where $\eta_k = \left[P_{\mathrm{B},k}G_{\mathrm{BU},k} r^{-\alpha_{\mathrm{BU},k}}\gamma_{\mathrm{th}}^{-1}\right]^{-1}$ *and* $\Phi(\cdot)$ *and* $g(\cdot)$ *are given by*

$$\Phi(p,q,w) = w^{2/q} + p^{2/q}\int_{\left(\frac{w}{p}\right)^{2/q}}^{\infty} \frac{\mathrm{d}x}{1 + x^{q/2}},$$

$$\begin{aligned}&F\left(\eta_k, \tau_k, k\right) \\ &= \exp\left\{-2\pi\lambda_{\mathrm{B},k}\int_{\tau_k}^{\infty}\left(\frac{e^{-\pi\lambda_{\mathrm{B},k} y^2}}{1 + \eta_k^{-1} P_{\max}^{-1} G_{\mathrm{UU},k}^{-1} z^{\alpha_{\mathrm{UU},k}}} \right.\right. \\ &\left.\left. + \int_0^{y^2} \frac{\pi\lambda_{\mathrm{B},k} e^{-\pi\lambda_{\mathrm{B},k} v}}{1 + \eta_k^{-1} p_k^{-1} G_{\mathrm{BU},k}^{\epsilon} v^{-\frac{1}{2}\epsilon\alpha_{\mathrm{BU},k}} G_{\mathrm{UU},k}^{-1} z^{\alpha_{\mathrm{UU},k}}}\,\mathrm{d}v\right) z\,\mathrm{d}z\right\}. \quad (14)\end{aligned}$$

where the lower limit of integration in (14)*, denoted as* τ_k*, is given by*

$$\begin{aligned}\tau_k &= \left(\frac{P_{\mathrm{B},1}G_{\mathrm{BU},1}}{P_{\mathrm{B},2}G_{\mathrm{BU},2}}\right)^{\frac{1}{\alpha_{\mathrm{BU},1}}} r^{\frac{\alpha_{\mathrm{BU},2}}{\alpha_{\mathrm{BU},1}}} \mathbb{1}\left\{k = 1, u \in \mathcal{U}_p\right\} \\ &+ \left(\frac{P_{\mathrm{B},2}G_{\mathrm{BU},2}\mathcal{B}}{P_{\mathrm{B},1}G_{\mathrm{BU},1}}\right)^{\frac{1}{\alpha_{\mathrm{BU},2}}} r^{\frac{\alpha_{\mathrm{BU},1}}{\alpha_{\mathrm{BU},2}}} \mathbb{1}\left\{k = 2, u \in \mathcal{U}_p\right\}. \quad (15)\end{aligned}$$

Proof: See Appendix B. ∎

Remark 1. *The DL coverage probability with resource partitioning is calculated using the expression provided in* (9)*. In contrast, when resource partitioning is not applied, the macrocells are assumed to be always active. In this case, a user associates with the strongest BS in the macrocells if* $P_{r,1} \geqslant \mathcal{B}P_{r,2}$*; otherwise, the user connects to the strongest BS* *in the picocells. Consequently, the probability of DL coverage without resource partition can be obtained using an analytical approach similar to that presented in this work.*

IV. Numerical Results

In this section, we validate the analytical results and examine the impact of various network parameters on the coverage probability. The simulation results are obtained by averaging over 10^5 independent system realizations. The system parameters are shown in Table I.

TABLE I
System Parameters

Parameter	Value
System Bandwidth	10 MHz
Thermal Noise Density	-174 dBm
Noise Figure	9 dB
ρ	-70 dBm
$\{\lambda_{\mathrm{B},1}, \lambda_{\mathrm{U}}\}$	$\{1, 100\}$BS/km^2
$\{\alpha_{\mathrm{BU},1}, \alpha_{\mathrm{BU},2}, \alpha_{\mathrm{UU},1}, \alpha_{\mathrm{UU},1}\}$	$\{3.5, 4, 4, 4\}$
$\{P_{\mathrm{B},1}, P_{\mathrm{B},2}\}$	$\{46, 26\}$dBm
$\{G_{\mathrm{BU},1}, G_{\mathrm{BU},2}, G_{\mathrm{UU},1}, G_{\mathrm{UU},2}\}$	$\{-40.4, -25.4, -55.78, -55.78\}$dB

Fig. 1 shows the DL coverage probability as a function of the association bias for selected values of picocell density and resource partitioning, with $\gamma_{\mathrm{th}} = -3$ dB and $\epsilon = 1$. As shown in the figure, users primarily associate with high-power macrocell BSs for small bias values, resulting in higher DL coverage probability. As the bias increases, a larger fraction of users is offloaded to low-power picocell BSs. In contrast, interference from active macrocell BSs increases, leading to a reduction in DL coverage probability. With resource partitioning, the coverage contribution from range-expanded users increases with bias, while the contribution from macrocell users decreases. In this case, muting macrocell transmissions reduces interference for users connected to picocell BSs, resulting in improved DL coverage probability compared to the scenario without resource partitioning. Additionally, as picocell density increases, interference on the orthogonal resources allocated to offloaded users increases, further decreasing DL coverage probability.

Fig. 2 illustrates the DL coverage probability as a function of the SINR threshold for $\mathcal{B} = 5$ dB, $\lambda_{\mathrm{B},2} = 5\lambda_{\mathrm{B},1}$, and selected values of ϵ. The figure indicates that as the SINR threshold increases, the DL coverage probability decreases. A higher SINR threshold makes it less likely for the downlink SINR to exceed the threshold, reducing the DL coverage probability. Additionally, as ϵ increases, the DL coverage probability decreases. This is because a higher ϵ leads to increased UL transmit power, which raises the total UL interference. In particular, when $\epsilon = 1$, the UE transmits at full power, causing more interference and resulting in lower DL coverage probability compared to the case when $\epsilon = 0$.

V. Conclusions

We studied an FD communication system consisting of two tiers, macrocells, and picocells, where BSs operate in FD mode while users operate in HD mode. The spatial distributions of

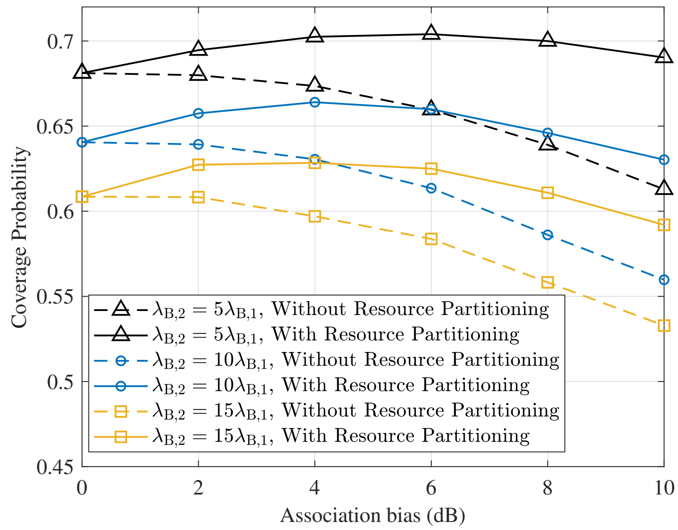

Fig. 1. The coverage probability is shown as a function of the association bias for selected values of picocell density, with and without resource partitioning, for $\gamma_{th} = -3$dB and $\epsilon = 1$.

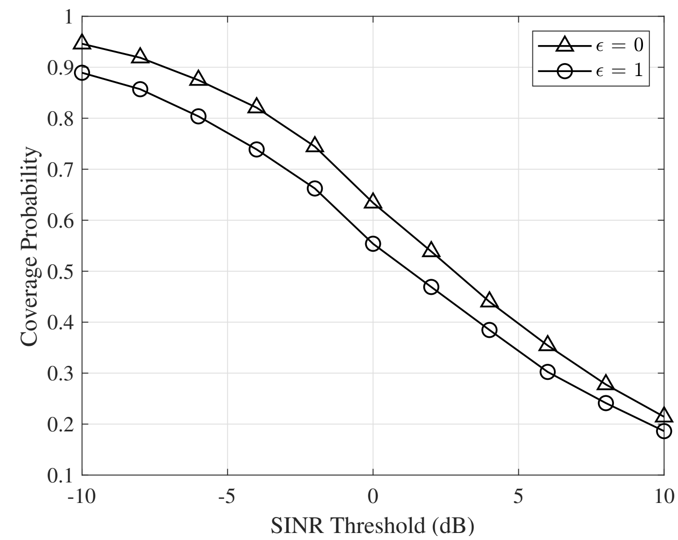

Fig. 2. The coverage probability as a function of the SINR threshold for $\mathcal{B} = 5$ dB, $\lambda_{\mathrm{B},2} = 5\lambda_{\mathrm{B},1}$, and selected values of ϵ.

BSs and users are modeled using independent 2D-PPP with constant intensity. All communication channels experience Rayleigh fading and path loss. We analyzed the effects of joint resource partitioning, offloading, and power control in the system and derived an analytical expression for the DL coverage probability. Our results show that load balancing alone is insufficient; when combined with offloading, resource partitioning is essential to improve DL coverage probability.

VI. Future Work

This study investigates performance enhancement in FD two-tier networks by employing user offloading and resource partitioning techniques to improve coverage probability. However, existing methods primarily focus on data transmission to enhance throughput and coverage probability, without considering the importance and relevance of the transmitted information. To address this limitation, a promising future research direction is the integration of semantics-aware performance metrics that account for the timeliness, relevance, and utility of information [20]–[29] in FD communication systems. In particular, we will examine metrics such as the Age of Information (AoI) [20], which more accurately capture the requirements of real-time and mission-critical applications. By shifting the performance evaluation focus from conventional throughput-based metrics to those reflecting the quality and usefulness of information delivery, this approach aims to provide a more comprehensive and application-aware assessment of network performance.

APPENDIX

A. Proof of Lemma 1

Using (4), the probability that the desired UE is associated with the macrocell, denoted as $\Pr\left[u \in \mathcal{U}_m\right]$, is given by

$$\begin{aligned}
&\Pr\left[u \in \mathcal{U}_m\right]\\
&=\Pr\left[P_{\mathrm{B},1}G_{\mathrm{BU},1}R_1^{-\alpha_{\mathrm{BU},1}} \geqslant \mathcal{B}P_{\mathrm{B},2}G_{\mathrm{BU},2}R_2^{-\alpha_{\mathrm{BU},2}}\right]\\
&=\Pr\left[R_2 \geqslant \left(\frac{P_{\mathrm{B},2}G_{\mathrm{BU},2}\mathcal{B}}{P_{\mathrm{B},1}G_{\mathrm{BU},1}}\right)^{\frac{1}{\alpha_{\mathrm{BU},2}}} R_1^{\frac{\alpha_{\mathrm{BU},1}}{\alpha_{\mathrm{BU},2}}}\right]\\
&=\int_0^\infty \Pr\left[R_2 \geqslant \left(\frac{P_{\mathrm{B},2}G_{\mathrm{BU},2}\mathcal{B}}{P_{\mathrm{B},1}G_{\mathrm{BU},1}}\right)^{\frac{1}{\alpha_{\mathrm{BU},2}}} r^{\frac{\alpha_{\mathrm{BU},1}}{\alpha_{\mathrm{BU},2}}}\middle| R_1 = r\right] f_{R_1}(r)\mathrm{d}r,
\end{aligned} \tag{16}$$

Using (1), we can simplify (16) as follows

$$\Pr\left[u \in \mathcal{U}_m\right] = \int_0^\infty 2\pi\lambda_{\mathrm{B},1} r \exp\left[-\pi\sum_{k=1}^{2}\lambda_{\mathrm{B},k} T_1^{\frac{2}{\alpha_{\mathrm{BU},k}}} r^{\frac{2\alpha_{\mathrm{BU},1}}{\alpha_{\mathrm{BU},k}}}\right]\mathrm{d}r, \tag{17}$$

where $T_1 = \frac{P_{\mathrm{B},k}G_{\mathrm{BU},k}\mathcal{B}^k}{P_{\mathrm{B},1}G_{\mathrm{BU},1}\mathcal{B}}$. Similarly, using (4), the probability that the desired UE is associated with a picocell, denoted as $\Pr\left[u \in \mathcal{U}p\right]$, and the probability that the desired UE is associated with a range-expanded picocell, denoted as $\Pr\left[u \in \mathcal{U}e\right]$, can be derived as follows:

$$\begin{aligned}
\Pr\left[u \in \mathcal{U}_p\right] &= \int_0^\infty 2\pi\lambda_{\mathrm{B},2} r \exp\left[-\pi\sum_{k=1}^{2}\lambda_{\mathrm{B},k} T_2^{\frac{2}{\alpha_{\mathrm{BU},k}}} r^{\frac{2\alpha_{\mathrm{BU},2}}{\alpha_{\mathrm{BU},2}}}\right]\mathrm{d}r,\\
\Pr\left[u \in \mathcal{U}_e\right] &= \int_0^\infty 2\pi\lambda_{\mathrm{B},2} r \left\{\exp\left[-\pi\sum_{k=1}^{2}\lambda_{\mathrm{B},k} T_3^{\frac{2}{\alpha_{\mathrm{BU},k}}} r^{\frac{2\alpha_{\mathrm{BU},2}}{\alpha_{\mathrm{BU},k}}}\right]\right.\\
&\qquad \left. -\exp\left[-\pi\sum_{k=1}^{2}\lambda_{\mathrm{B},k} T_2^{\frac{2}{\alpha_{\mathrm{BU},k}}} r^{\frac{2\alpha_{\mathrm{BU},2}}{\alpha_{\mathrm{BU},k}}}\right]\right\}\mathrm{d}r,
\end{aligned} \tag{18}$$

where $T_2 = \frac{P_{\mathrm{B},k}G_{\mathrm{BU},k}}{P_{\mathrm{B},2}G_{\mathrm{BU},2}}$, and $T_3 = \frac{P_{\mathrm{B},k}G_{\mathrm{BU},k}\mathcal{B}^k}{P_{\mathrm{B},2}G_{\mathrm{BU},2}\mathcal{B}^2}$.

B. Proof of Lemma 2

Using (5), we can obtain the first conditional probability in (9) as

$$\begin{aligned}
&\Pr\left[\mathrm{SINR} > \gamma_{\mathrm{th}} \mid u \in \mathcal{U}_m\right]\\
&= \Pr\left[\frac{P_{\mathrm{B},1}H_o G_{\mathrm{BU},1}R_1^{-\alpha_{\mathrm{BU},1}}}{\sum_{k=1}^{2} I_{m,k} + \sigma_{\mathrm{U}}^2} > \gamma_{\mathrm{th}}\middle| u \in \mathcal{U}_m\right].
\end{aligned} \tag{19}$$

Using total probability theorem, (19) can be written as

$$\begin{aligned}
&\Pr\left[\frac{P_{\mathrm{B},1}H_{\mathrm{o}}G_{\mathrm{BU},1}R_1^{-\alpha_{\mathrm{BU},1}}}{\sum_{k=1}^{2} I_{m,k} + \sigma_{\mathrm{U}}^2} > \gamma_{\mathrm{th}}\middle| u \in \mathcal{U}_{\mathrm{m}}\right]\\
&= \int_0^\infty \Pr\left[\frac{P_{\mathrm{B},1}H_{\mathrm{o}}G_{\mathrm{BU},1}r^{-\alpha_{\mathrm{BU},1}}}{\sum_{k=1}^{2} I_{m,k} + \sigma_{\mathrm{U}}^2} > \gamma_{\mathrm{th}}\middle| u \in \mathcal{U}_m, R_1 = r\right]\\
&\qquad \times f_{R_1}\left(r \middle| u \in \mathcal{U}_m\right)\mathrm{d}r.
\end{aligned} \tag{20}$$

The first term in the integral in (20) can be expressed as

$$\begin{aligned}
&\Pr\left[\frac{P_{\mathrm{B},1}H_{\mathrm{o}}G_{\mathrm{BU},1}r^{-\alpha_{\mathrm{BU},1}}}{\sum_{k=1}^{2} I_{m,k} + \sigma_{\mathrm{U}}^2} > \gamma_{\mathrm{th}}\middle| u \in \mathcal{U}_m, R_1 = r\right]\\
&= \Pr\left[H_{\mathrm{o}} > \left(P_{\mathrm{B},1}G_{\mathrm{BU},1}r^{-\alpha_{\mathrm{BU},1}}\gamma_{\mathrm{th}}^{-1}\right)^{-1}\left[\sum_{k=1}^{2} I_{m,k} + \sigma_{\mathrm{U}}^2\right]\right]\\
&= \mathbb{E}\left\{\exp\left(-\left[P_{\mathrm{B},1}G_{\mathrm{BU},1}r^{-\alpha_{\mathrm{BU},1}}\gamma_{\mathrm{th}}^{-1}\right]^{-1}\left[\sum_{k=1}^{2} I_{m,k} + \sigma_{\mathrm{U}}^2\right]\right)\right\}\\
&= \exp\left(-\left[P_{\mathrm{B},1}G_{\mathrm{BU},1}r^{-\alpha_{\mathrm{BU},1}}\gamma_{\mathrm{th}}^{-1}\right]^{-1}\sigma_{\mathrm{U}}^2\right)\\
&\quad \times \prod_{k=1}^{2}\mathbb{E}_{I_{m,k}}\left\{\exp\left(-\left[P_{\mathrm{B},1}G_{\mathrm{BU},1}r^{-\alpha_{\mathrm{BU},1}}\gamma_{\mathrm{th}}^{-1}\right]^{-1} I_{m,k}\right)\right\}\\
&= \exp\left(-\left[P_{\mathrm{B},1}G_{\mathrm{BU},1}r^{-\alpha_{\mathrm{BU},1}}\gamma_{\mathrm{th}}^{-1}\right]^{-1}\sigma_{\mathrm{U}}^2\right)\\
&\quad \times \prod_{k=1}^{2}\mathcal{L}_{I_{m,k}}\left(\left[P_{\mathrm{B},1}G_{\mathrm{BU},1}r^{-\alpha_{\mathrm{BU},1}}\gamma_{\mathrm{th}}^{-1}\right]^{-1}\right),
\end{aligned} \tag{21}$$

where $\mathcal{L}_{I_{m,k}}(s)$ denote the Laplace transform of the total interference $I_{m,k}$, evaluated at $s = \left[P_{\mathrm{B},1}G_{\mathrm{BU},1}r^{-\alpha_{\mathrm{BU},1}}\gamma_{\mathrm{th}}^{-1}\right]^{-1}$. Using (6), (7), and (8), one can obtain $\mathcal{L}_{I_{m,k}}(s)$ as

$$\begin{aligned}
&\mathcal{L}_{I_{m,k}}(s)\\
&= \mathbb{E}_{L_j,R_j,D_j,H_j,Q_j}\left\{\exp\left[-s\left(\sum_{\mathrm{B}_j\in\Phi_{\mathrm{B},k}\setminus\{\mathrm{B}_{\mathrm{o}}\}} P_{\mathrm{B},k}G_{\mathrm{BU},k}H_j L_j^{-\alpha_{\mathrm{BU},k}}\right.\right.\right.\\
&\quad \left.\left.\left. + \sum_{u_j\in\Phi_{\mathrm{U},k}\setminus\{u_{\mathrm{o}}\}} P_{\mathrm{U},k}\left(R_j\right)G_{\mathrm{UU},k}\mathcal{Q}_j D_j^{-\alpha_{\mathrm{UU},k}}\right)\right]\right\}.
\end{aligned} \tag{22}$$

According to the independence among L_j, R_j, and D_j mentioned in Section II, one can write (22) as

$$\begin{aligned}
&\mathcal{L}_{I_{m,k}}(s)\\
&= \mathbb{E}_{L_j,H_j}\left\{\exp\left[-s\left(\sum_{\mathrm{B}_j\in\Phi_{\mathrm{B},k}\setminus\{\mathrm{B}_{\mathrm{o}}\}} P_{\mathrm{B},k}G_{\mathrm{BU},k}H_j L_j^{-\alpha_{\mathrm{BU},k}}\right)\right]\right\}\\
&\times \mathbb{E}_{R_j,D_j,Q_j}\left\{\exp\left[-s\left(\sum_{u_j\in\Phi_{\mathrm{U},k}\setminus\{u_{\mathrm{o}}\}} P_{\mathrm{U},k}(R_j)G_{\mathrm{UU},k}Q_j D_j^{-\alpha_{\mathrm{UU},k}}\right)\right]\right\}.
\end{aligned} \tag{23}$$

The expression in (23) is simplified as

$$
\begin{aligned}
&\mathcal{L}_{I_{m,k}}(s)\\
&=\mathbb{E}_{L_j}\Bigg\{\prod_{\mathrm{B}_j\in\Phi_{\mathrm{B},k}\setminus\{\mathrm{B_o}\}}\mathbb{E}_{H_j}\Big\{\exp\Big[-sP_{\mathrm{B},k}G_{\mathrm{BU},k}H_jL_j^{-\alpha_{\mathrm{BU},k}}\Big]\Big\}\Bigg\}\\
&\times\mathbb{E}_{R_j,D_j}\Bigg\{\prod_{u_j\in\Phi_{\mathrm{U},k}\setminus\{u_\mathrm{o}\}}\mathbb{E}_{Q_j}\Big\{\exp\Big[-sP_{\mathrm{U},k}(R_j)G_{\mathrm{UU},k}Q_jD_j^{-\alpha_{\mathrm{UU},k}}\Big]\Big\}\Bigg\}\\
&=\mathbb{E}_{L_j}\Bigg\{\prod_{\mathrm{B}_j\in\Phi_{\mathrm{B},k}\setminus\{\mathrm{B_o}\}}\mathcal{L}_{H_j}\left(sP_{\mathrm{B},k}G_{\mathrm{BU},k}L_j^{-\alpha_{\mathrm{BU},k}}\right)\Bigg\}\\
&\times\mathbb{E}_{R_j,D_j}\Bigg\{\prod_{u_j\in\Phi_{\mathrm{U},k}\setminus\{u_\mathrm{o}\}}\mathcal{L}_{Q_j}\left(sP_{\mathrm{U},k}\left(R_j\right)G_{\mathrm{UU},k}D_j^{-\alpha_{\mathrm{UU},k}}\right)\Bigg\}.
\end{aligned}\tag{24}
$$

Now, using the Probability Generating Functional (PGFL) of a PPP [30], (24) can be written as

$$
\begin{aligned}
&\mathcal{L}_{I_{m,k}}(s)\\
&=\exp\Big\{-2\pi\lambda_{\mathrm{B},k}\int_{x_k}^{\infty}\left[1-\mathcal{L}_{H_j}\left(sP_{\mathrm{B},k}G_{\mathrm{BU},k}\varrho^{-\alpha_{\mathrm{BU},k}}\right)\right]\varrho\mathrm{d}\varrho\Big\}\\
&\times\exp\Big\{-2\pi\lambda_{\mathrm{B},k}\int_{\tau_k}^{\infty}\mathbb{E}_{R_j}\big[1-\mathcal{L}_{Q_j}\big(sP_{\mathrm{U},k}(R_j)G_{\mathrm{UU},k}z^{-\alpha_{\mathrm{UU},k}}\big)\big]z\mathrm{d}z\Big\}\\
&=\exp\left\{-2\pi\lambda_{\mathrm{B},k}\int_{x_k}^{\infty}\frac{\varrho}{1+\left(sP_{\mathrm{B},k}G_{\mathrm{BU},k}\right)^{-1}\varrho^{\alpha_{\mathrm{BU},k}}}\,\mathrm{d}\varrho\right\}\\
&\times\exp\Bigg\{-2\pi\lambda_{\mathrm{B},k}\int_{\tau_k}^{\infty}\Bigg(\frac{\pi\lambda_{\mathrm{B},k}e^{-\pi\lambda_{\mathrm{B},k}y^2}}{1+s^{-1}P_{\max}^{-1}G_{\mathrm{UU},k}^{-1}z^{\alpha_{\mathrm{UU},k}}}\\
&+\int_0^{y^2}\frac{\pi\lambda_{\mathrm{B},k}e^{-\pi\lambda_{\mathrm{B},k}v}}{1+s^{-1}p_k^{-1}G_{\mathrm{BU},k}^{\epsilon}v^{-\frac{1}{2}\epsilon\alpha_{\mathrm{BU},k}}G_{\mathrm{UU},k}^{-1}z^{\alpha_{\mathrm{UU},k}}}\,\mathrm{d}v\Bigg)z\,\mathrm{d}z\Bigg\},
\end{aligned}\tag{25}
$$

where y in (25) is given by (2). Using (4), the lower limits of the integrals in (25) can be determined as follows:

$$
x_k=\begin{cases}
r & ,k=1,u\in\mathcal{U}_m\\
\left(\frac{P_{\mathrm{B},1}G_{\mathrm{BU},1}}{P_{\mathrm{B},2}G_{\mathrm{BU},2}}\right)^{\frac{1}{\alpha_{\mathrm{BU},1}}}r^{\frac{\alpha_{\mathrm{BU},2}}{\alpha_{\mathrm{BU},1}}} & ,k=1,u\in\mathcal{U}_p\\
\left(\frac{P_{\mathrm{B},2}G_{\mathrm{BU},2}\mathcal{B}}{P_{\mathrm{B},1}G_{\mathrm{BU},1}}\right)^{\frac{1}{\alpha_{\mathrm{BU},2}}}r^{\frac{\alpha_{\mathrm{BU},1}}{\alpha_{\mathrm{BU},2}}} & ,k=2,u\in\mathcal{U}_m\\
r & ,k=2,u\in\mathcal{U}_p\\
r & ,k=2,u\in\mathcal{U}_e,
\end{cases}\tag{26}
$$

$$
\tau_k=\begin{cases}
0 & ,k=1,u\in\mathcal{U}_m\\
\left(\frac{P_{\mathrm{B},1}G_{\mathrm{BU},1}}{P_{\mathrm{B},2}G_{\mathrm{BU},2}}\right)^{\frac{1}{\alpha_{\mathrm{BU},1}}}r^{\frac{\alpha_{\mathrm{BU},2}}{\alpha_{\mathrm{BU},1}}} & ,k=1,u\in\mathcal{U}_p\\
\left(\frac{P_{\mathrm{B},2}G_{\mathrm{BU},2}\mathcal{B}}{P_{\mathrm{B},1}G_{\mathrm{BU},1}}\right)^{\frac{1}{\alpha_{\mathrm{BU},2}}}r^{\frac{\alpha_{\mathrm{BU},1}}{\alpha_{\mathrm{BU},2}}} & ,k=2,u\in\mathcal{U}_m\\
0 & ,k=2,u\in\mathcal{U}_p\\
0 & ,k=2,u\in\mathcal{U}_e.
\end{cases}\tag{27}
$$

Now, By applying the change of variables $x=(sP_{\mathrm{B},k}G_{\mathrm{BU},k})^{\frac{-2}{\alpha_{\mathrm{BU},k}}}\varrho^2$, the Laplace transform $\mathcal{L}_{I_{m,k}}(s)$ can be expressed as:

$$
\begin{aligned}
&\mathcal{L}_{I_{m,k}}(s)=\exp\Bigg\{-\pi\lambda_{\mathrm{B},k}\left(sP_{\mathrm{B},k}G_{\mathrm{BU},k}\right)^{\frac{2}{\alpha_{\mathrm{BU},k}}}\\
&\times\int_{x_k^2(sP_{\mathrm{B},k}G_{\mathrm{BU},k})^{\frac{-2}{\alpha_{\mathrm{BU},k}}}}^{\infty}\frac{1}{1+x^{\frac{1}{2}\alpha_{\mathrm{BU},k}}}\,\mathrm{d}x\Bigg\}\\
&\times\exp\Bigg\{-2\pi\lambda_{\mathrm{B},k}\int_{\tau_k}^{\infty}\Bigg(\frac{e^{-\pi\lambda_{\mathrm{B},k}y^2}}{1+s^{-1}P_{\max}^{-1}G_{\mathrm{UU},k}^{-1}z^{\alpha_{\mathrm{UU},k}}}\\
&+\int_0^{y^2}\frac{\pi\lambda_{\mathrm{B},k}e^{-\pi\lambda_{\mathrm{B},k}v}}{1+s^{-1}p_k^{-1}G_{\mathrm{BU},k}^{\epsilon}v^{-\frac{1}{2}\epsilon\alpha_{\mathrm{BU},k}}G_{\mathrm{UU},k}^{-1}z^{\alpha_{\mathrm{UU},k}}}\,\mathrm{d}v\Bigg)z\,\mathrm{d}z\Bigg\}.
\end{aligned}\tag{28}
$$

Now, we proceed to obtain $f_{R_1}\left(r\mid u\in\mathcal{U}_\mathrm{m}\right)$ as given in (20). To derive $f_{R_1}\left(r\mid u\in\mathcal{U}_\mathrm{m}\right)$, we first calculate the conditional cumulative distribution function (CDF) of r as follows:

$$
\begin{aligned}
F_{R_1}(r|u\in\mathcal{U}_m)&=\frac{\Pr[R_1\leqslant r,u\in\mathcal{U}_m]}{\Pr[u\in\mathcal{U}_m]}\\
&=\frac{\Pr[R_1\leqslant r,P_{\mathrm{B},1}G_{\mathrm{BU},1}R_1^{-\alpha_{\mathrm{BU},1}}\geqslant\mathcal{B}P_{\mathrm{B},2}G_{\mathrm{BU},2}R_2^{-\alpha_{\mathrm{BU},2}}]}{\Pr[u\in\mathcal{U}_m]}\\
&=\frac{1}{\Pr[u\in\mathcal{U}_m]}\int_0^r\Pr\left[R_2\geqslant\left(\frac{P_{\mathrm{B},2}G_{\mathrm{BU},2}\mathcal{B}}{P_{\mathrm{B},1}G_{\mathrm{BU},1}}\right)^{\frac{1}{\alpha_{\mathrm{BU},2}}}x^{\frac{\alpha_{\mathrm{BU},1}}{\alpha_{\mathrm{BU},2}}}\right]f_{R_1}(r)\mathrm{d}r.
\end{aligned}\tag{29}
$$

Using (1), we can simplify (29) as follows

$$
\begin{aligned}
&F_{R_1}(r|u\in\mathcal{U}_m)\\
&=\frac{2\pi\lambda_{\mathrm{B},1}}{\Pr[u\in\mathcal{U}_m]}\int_0^r x\exp\left[-\pi\sum_{k=1}^{2}\lambda_{\mathrm{B},k}\left(\frac{P_{\mathrm{B},k}G_{\mathrm{BU},k}\mathcal{B}^k}{P_{\mathrm{B},1}G_{\mathrm{BU},1}\mathcal{B}}\right)^{\frac{2}{\alpha_{\mathrm{BU},k}}}x^{\frac{2\alpha_{\mathrm{BU},1}}{\alpha_{\mathrm{BU},k}}}\right]\mathrm{d}x.
\end{aligned}\tag{30}
$$

Taking the derivative of (30) with respect to r, we obtain $f_{R_1}\left(r\mid u\in\mathcal{U}_m\right)$ as

$$
\begin{aligned}
&f_{R_1}\left(r\mid u\in\mathcal{U}_m\right)\\
&=\frac{2\pi\lambda_{\mathrm{B},1}r}{\Pr\left[u\in\mathcal{U}_m\right]}\exp\left[-\pi\sum_{k=1}^{2}\lambda_{\mathrm{B},k}\left(\frac{P_{\mathrm{B},k}G_{\mathrm{BU},k}\mathcal{B}^k}{P_{\mathrm{B},1}G_{\mathrm{BU},1}\mathcal{B}}\right)^{\frac{2}{\alpha_{\mathrm{BU},k}}}r^{\frac{2\alpha_{\mathrm{BU},1}}{\alpha_{\mathrm{BU},k}}}\right].
\end{aligned}\tag{31}
$$

Using (22), (28), and (31), we can express (20) as:

$$
\begin{aligned}
&\Pr\left[\mathrm{SINR}>\gamma_{\mathrm{th}}\middle|u\in\mathcal{U}_m\right]\\
&=\int_0^{\infty}\frac{2\pi\lambda_{\mathrm{B},1}r}{\Pr\left[u\in\mathcal{U}_m\right]}\exp\Bigg[-\Bigg(\pi\sum_{k=1}^{2}\lambda_{\mathrm{B},k}\left(\frac{P_{\mathrm{B},k}G_{\mathrm{BU},k}}{P_{\mathrm{B},1}G_{\mathrm{BU},1}}\right)^{\frac{2}{\alpha_{\mathrm{BU},k}}}r^{\frac{2\alpha_{\mathrm{BU},1}}{\alpha_{\mathrm{BU},k}}}\\
&\times\Phi\left(\gamma_{\mathrm{th}},\alpha_{\mathrm{BU},k},\frac{\mathcal{B}^k}{\mathcal{B}}\right)+\eta_1\sigma_{\mathrm{U}}^2\Bigg)\Bigg]\prod_{k=1}^{2}g\left(\eta_1,\tau_k,k\right)\mathrm{d}r.
\end{aligned}\tag{32}
$$

where $\eta_k = \left[P_{\mathrm{B},k} G_{\mathrm{BU},k} r^{-\alpha_{\mathrm{BU},k}} \gamma_{\mathrm{th}}^{-1}\right]^{-1}$ and

$$\Phi(p,q,w) = w^{2/q} + p^{2/q} \int_{\left(\frac{w}{p}\right)^{2/q}}^{\infty} \frac{\mathrm{d}x}{1+x^{q/2}},$$

$$\begin{aligned} & g\left(\eta_k, \tau_k, k\right) \\ & = \exp\Bigg\{ -2\pi\lambda_{\mathrm{B},k} \int_{\tau_k}^{\infty} \Bigg(\frac{e^{-\pi\lambda_{\mathrm{B},k} y^2}}{1+\eta_k^{-1} P_{\max}^{-1} G_{\mathrm{UU},k}^{-1} z^{\alpha_{\mathrm{UU},k}}} \\ & + \int_0^{y^2} \frac{\pi\lambda_{\mathrm{B},k} e^{-\pi\lambda_{\mathrm{B},k} v}}{1+\eta_k^{-1} p_k^{-1} G_{\mathrm{BU},k}^{\epsilon} v^{-\frac{1}{2}\epsilon\alpha_{\mathrm{BU},k}} G_{\mathrm{UU},k}^{-1} z^{\alpha_{\mathrm{UU},k}}} \,\mathrm{d}v \Bigg) z \,\mathrm{d}z \Bigg\}. \end{aligned} \tag{33}$$

Using the similar procedure led to (32), we can obtain the second and third conditional probabilities in (9) as

$$\begin{aligned} & \Pr\left[\text{SINR} > \gamma_{\text{th}} \middle| u \in \mathcal{U}_p\right] \\ & = \int_0^{\infty} \frac{2\pi\lambda_{\mathrm{B},2} r}{\Pr\left[u \in \mathcal{U}_p\right]} \exp\Bigg[-\Bigg(\pi \sum_{k=1}^{2} \lambda_{\mathrm{B},k} T_2^{\frac{2}{\alpha_{\mathrm{BU},k}}} r^{\frac{2\alpha_{\mathrm{BU},2}}{\alpha_{\mathrm{BU},k}}} \\ & \times \Phi\left(\gamma_{\mathrm{th}}, \alpha_{\mathrm{BU},k}, 1\right) + \eta_2 \sigma_{\mathrm{U}}^2 \Bigg) \Bigg] \prod_{k=1}^{2} g\left(\eta_2, \tau_k, k\right) \mathrm{d}r, \end{aligned} \tag{34}$$

$$\begin{aligned} & \Pr\left[\text{SINR} > \gamma_{\text{th}} \middle| u \in \mathcal{U}_e\right] \\ & = \int_0^{\infty} \frac{2\pi\lambda_{\mathrm{B},2} r}{\Pr\left[u \in \mathcal{U}_e\right]} \exp\left[-\left(\pi\lambda_{\mathrm{B},2} r^2 \Phi\left(\gamma_{\mathrm{th}}, \alpha_{\mathrm{BU},2}, 1\right) + \eta_2 \sigma_{\mathrm{U}}^2\right)\right] \\ & \times \Bigg\{ \exp\left[-\pi\lambda_{\mathrm{B},1} \left(\frac{P_{\mathrm{B},1} G_{\mathrm{BU},1}}{P_{\mathrm{B},2} G_{\mathrm{BU},2} \mathcal{B}} \right)^{\frac{2}{\alpha_{\mathrm{BU},1}}} r^{\frac{2\alpha_{\mathrm{BU},2}}{\alpha_{\mathrm{BU},1}}} \right] \\ & - \exp\left[-\pi\lambda_{\mathrm{B},1} \left(\frac{P_{\mathrm{B},1} G_{\mathrm{BU},1}}{P_{\mathrm{B},2} G_{\mathrm{BU},2}} \right)^{\frac{2}{\alpha_{\mathrm{BU},1}}} r^{\frac{2\alpha_{\mathrm{BU},2}}{\alpha_{\mathrm{BU},1}}} \right] \Bigg\} g\left(\eta_2, \tau_2, k\right) \mathrm{d}r. \end{aligned} \tag{35}$$

References

[1] H.-S. Jo, C. Mun, J. Moon, and J.-G. Yook, "Interference mitigation using uplink power control for two-tier femtocell networks," *IEEE transactions on wireless communications*, vol. 8, no. 10, pp. 4906–4910, 2009.

[2] ——, "Self-optimized coverage coordination in femtocell networks," *IEEE Transactions on Wireless Communications*, vol. 9, no. 10, pp. 2977–2982, 2010.

[3] A. Damnjanovic, J. Montojo, Y. Wei, T. Ji, T. Luo, M. Vajapeyam, T. Yoo, O. Song, and D. Malladi, "A survey on 3GPP heterogeneous networks," *IEEE Wireless communications*, vol. 18, no. 3, pp. 10–21, 2011.

[4] A. Ghosh, N. Mangalvedhe, R. Ratasuk, B. Mondal, M. Cudak, E. Visotsky, T. A. Thomas, J. G. Andrews, P. Xia, H. S. Jo *et al.*, "Heterogeneous cellular networks: From theory to practice," *IEEE communications magazine*, vol. 50, no. 6, pp. 54–64, 2012.

[5] R. Madan, J. Borran, A. Sampath, N. Bhushan, A. Khandekar, and T. Ji, "Cell association and interference coordination in heterogeneous LTE-A cellular networks," *IEEE Journal on selected areas in communications*, vol. 28, no. 9, pp. 1479–1489, 2010.

[6] S. Singh, J. G. Andrews, and G. de Veciana, "Interference shaping for improved quality of experience for real-time video streaming," *IEEE Journal on Selected Areas in Communications*, vol. 30, no. 7, pp. 1259–1269, 2012.

[7] D. Lopez-Perez, I. Guvenc, G. De la Roche, M. Kountouris, T. Q. Quek, and J. Zhang, "Enhanced intercell interference coordination challenges in heterogeneous networks," *IEEE Wireless communications*, vol. 18, no. 3, pp. 22–30, 2011.

[8] S. Mukherjee and I. Güvenç, "Effects of range expansion and interference coordination on capacity and fairness in heterogeneous networks," in *2011 Conference Record of the Forty Fifth Asilomar Conference on Signals, Systems and Computers (ASILOMAR)*, 2011, pp. 1855–1859.

[9] T. D. Novlan, R. K. Ganti, A. Ghosh, and J. G. Andrews, "Analytical evaluation of fractional frequency reuse for heterogeneous cellular networks," *IEEE Transactions on Communications*, vol. 60, no. 7, pp. 2029–2039, 2012.

[10] S. Singh and J. G. Andrews, "Joint resource partitioning and offloading in heterogeneous cellular networks," *IEEE Transactions on Wireless Communications*, vol. 13, no. 2, pp. 888–901, 2014.

[11] J. G. Andrews, S. Buzzi, W. Choi, S. V. Hanly, A. Lozano, A. C. Soong, and J. C. Zhang, "What will 5G be?" *IEEE Journal on selected areas in communications*, vol. 32, no. 6, pp. 1065–1082, 2014.

[12] S. Goyal, P. Liu, S. Panwar, R. Yang, R. A. DiFazio, and E. Bala, "Full duplex operation for small cells," *arXiv preprint arXiv:1412.8708*, 2014.

[13] S. Goyal, P. Liu, S. S. Panwar, R. A. Difazio, R. Yang, and E. Bala, "Full duplex cellular systems: will doubling interference prevent doubling capacity?" *IEEE Communications Magazine*, vol. 53, no. 5, pp. 121–127, 2015.

[14] J. Lee and T. Q. Quek, "Hybrid full-/half-duplex system analysis in heterogeneous wireless networks," *IEEE transactions on wireless communications*, vol. 14, no. 5, pp. 2883–2895, 2015.

[15] H.-F. Arraño-Scharager, J.-M. Kelif, and M. Coupechoux, "Performance evaluation of millimeter wave full-duplex cellular networks," in *2018 IEEE Globecom Workshops (GC Wkshps)*, 2018, pp. 1–7.

[16] J. G. Andrews, F. Baccelli, and R. K. Ganti, "A tractable approach to coverage and rate in cellular networks," *IEEE Transactions on communications*, vol. 59, no. 11, pp. 3122–3134, 2011.

[17] W. Xiao, R. Ratasuk, A. Ghosh, R. Love, Y. Sun, and R. Nory, "Uplink power control, interference coordination and resource allocation for 3GPP E-UTRA," in *IEEE Vehicular Technology Conference*, 2006, pp. 1–5.

[18] A. H. Sakr and E. Hossain, "On user association in multi-tier full-duplex cellular networks," *IEEE Transactions on Communications*, vol. 65, no. 9, pp. 4080–4095, 2017.

[19] L. Barolli, F. Xhafa, A. Durresi, and A. Koyama, "A fuzzy-based handover system for avoiding ping-pong effect in wireless cellular networks," in *2008 International conference on parallel processing-workshops*, 2008, pp. 135–142.

[20] R. D. Yates, Y. Sun, D. R. Brown, S. K. Kaul, E. Modiano, and S. Ulukus, "Age of Information: An Introduction and Survey," *IEEE Journal on Selected Areas in Communications*, vol. 39, no. 5, pp. 1183–1210, 2021.

[21] N. Pappas, M. A. Abd-Elmagid, B. Zhou, W. Saad, and H. S. Dhillon, *Age of Information: Foundations and Applications*. Cambridge University Press, 2023.

[22] M. Kountouris and N. Pappas, "Semantics-empowered communication for networked intelligent systems," *IEEE Communications Magazine*, vol. 59, no. 6, pp. 96–102, 2021.

[23] A. Maatouk, S. Kriouile, M. Assaad, and A. Ephremides, "The age of incorrect information: A new performance metric for status updates," *IEEE/ACM Transactions on Networking*, vol. 28, no. 5, pp. 2215–2228, 2020.

[24] N. Pappas and M. Kountouris, "Goal-oriented communication for real-time tracking in autonomous systems," in *2021 IEEE International Conference on Autonomous Systems (ICAS)*, 2021, pp. 1–5.

[25] M. Salimnejad, M. Kountouris, and N. Pappas, "Real-time reconstruction of markov sources and remote actuation over wireless channels," *IEEE Transactions on Communications*, vol. 72, no. 5, pp. 2701–2715, 2024.

[26] ——, "State-aware real-time tracking and remote reconstruction of a markov source," *Journal of Communications and Networks*, vol. 25, no. 5, pp. 657–669, 2023.

[27] M. Salimnejad, M. Kountouris, A. Ephremides, and N. Pappas, "Age of information versions: a semantic view of markov source monitoring," *arXiv preprint arXiv:2406.14594*, 2024.

[28] ——, "Version Innovation Age and Age of Incorrect Version for Monitoring Markovian Sources," in *2024 22nd International Symposium on Modeling and Optimization in Mobile, Ad Hoc, and Wireless Networks (WiOpt)*, 2024, pp. 162–169.

[29] E. Delfani and N. Pappas, "Version age-optimal cached status updates in a gossiping network with energy harvesting sensor," *IEEE Transactions on Communications*, vol. 73, no. 4, pp. 2344–2360, 2025.

[30] S. N. Chiu, D. Stoyan, W. S. Kendall, and J. Mecke, *Stochastic geometry and its applications*. John Wiley & Sons, 2013.